Investigation of physical properties of spin coated $Ni_{1-x}Zn_xO$ (x = 0, 0.05, 0.07, 0.09) thin films for application as hole transport layer for perovskite solar cells

M. Abbas [a], M. Haseeb-u-Rehman [a], M. Sohail [b], G. H. Tariq [a,*]
[a] *Photovoltaic and renewable energy laboratory (PRE-Lab), Institute of Physics, Khawaja Fareed University of Engineering and Information Technology, Rahim Yar Khan 64200, Pakistan*
[b] *Department of Life Sciences, Khawaja Fareed University of Engineering and Information Technology, Rahim Yar Khan 64200, Pakistan*

The unique physical properties of the inorganic NiO thin film make it a more appealing candidate for use as a hole transport layer. However, these physical properties are strongly influenced by doping a semiconductor into a NiO lattice. In this study, we inspected the doping effects of zinc on the structural, optical, morphological, and electrical properties of the $Ni_{1-x}Zn_xO$ thin films fabricated via spin-coating technique, demonstrating their potential as hole transport layers. XRD spectra exhibited a small (200) peak with low intensity, indicating weak crystallinity in the pure NiO and zinc doped NiO thin film. FTIR spectra revealed the existence of the Ni-O groups at four bending positions (456 cm^{-1}, 446 cm^{-1}, 450 cm^{-1}, and 451 cm^{-1}). UV-visible spectra analysis revealed an increase in bandgap energy from 3.88 eV to 3.98 eV with the enhancement of zinc concentration from 0 to 0.09. The homogeneous morphology hidden within pure and doped NiO thin films was investigated using scanning electron microscopy. The Hall effect tests revealed that adding zinc to pure NiO thin film increased carrier concentration and decreased resistivity.

(Received December 18, 2024; Accepted February 18, 2025)

Keywords: $Ni_{1-x}Zn_xO$, Thin films, FTIR, Optical transmittance, Conductivity type, Hole transport layer

1. Introduction

Scientists are keenly interested in optimizing the electrical, optical, and structural properties of the charge-transporting layers of the perovskite solar cells (PSCs). Optimizing these physical characteristics has helped scientists to enhance the efficiency of the PSCs up to 26.4% [1]. PSCs are being recognized as the future of the solar cell technology due to their exceptional photo conversion efficiency and ease of manufacturing The remarkable optoelectronic properties of PSCs are likely to make them commercially viable shortly [2]. The three primary components of perovskite solar cells are the hole transport layer (HTL), the electron transport layer (ETL), and the perovskite layer itself. The perovskite layer is responsible for absorbing sunlight, leading to the creation of electron-hole pairs. The ETL is designed to selectively move the electrons toward one of the electrodes, while the HTL is tasked with transporting the holes to opposite electrode, simultaneously preventing recombination of electrons. Furthermore, the HTL helps in aligning the energy levels between the perovskite layer and its adjacent electrode. This makes the role of the HTL crucial in efficiently extracting the photo-generated holes and ensuring they reach the electrode, significantly influencing the overall efficacy of the PSCs.

Several metal oxides including CuO, NiO_x, VO_x, WO_x, and MoO_x, are frequently used in the fabrication of the p-type HTL [3]. NiO is a unique metal oxide in comparison to other metal oxides with a broad band gap [4], variable valence states (Ni^3, Ni^{2+}) [5], high melting and boiling temperature, strong chemical and thermal stability, and p-type conductivity [6]. With a high tuneable work function of 3.7 eV to 6.7 eV [7, 8] which ensures an efficient charge transportation. Therefore, NiO with these exceptional properties has more potential be used as material in the creation of hole

* Corresponding author: hasnain.tariq@kfueit.edu.pk
https://doi.org/10.15251/JOR.2025.211.151

transport layers (HTLs) for application in PSCs. In addition to this, NiO thin films have a wide range of applications such as magnetic memory devices, solar cells, nano-electronic devices, sensors, electromagnetic absorbers [9], supercapacitors, photo-catalysts, and spintronic devices [10].

Doping different elements in the NiO thin films fabricated via different coating methods can lead to enchantments in the structural, morphological, and electrical properties [11, 12], making them acceptable for required applications. Using the RF sputtering coating technique, Manouchehri and co-workers prepared NiO thin films, and reported that the band gap of the NiO reduced as Zn doping increased [13]. Amor and with his team mates used the spray-pyrolysis method to create NiO thin films and demonstrated that the band gap widened from 3.59 eV to 3.63 eV with the addition of 2% Mg doping. They demonstrated numerous improvements in the structure, making the Mg-doped NiO thin films suitable for microelectronics applications [14]. During the research conducted by Sen and colleagues, demonstrated that the surface roughness first rose from 4 nm to 6.08 nm with an increase in zinc concentration, but when the concentration of zinc continued to climb, it reduced to 5.72 nm [15]. Fei Wang and colleagues prepared thin films using magnetron sputtering method, and they demonstrated that doping of the zinc in NiO thin films significantly increases the cycling stability of the thin films and they achieved colouration efficiency of 11.20 cm^2/C. Zinc addition to the NiO thin films also resulted a decrease of the charge transfer resistance [16]. Using an electron beam evaporation method, Denny and co-workers inspected the improvements in the NiO thin films' electrical characteristics while preserving the substance's p-type conductivity and showed that optical band gap decreased by Na doping [17]. Aydin and his team employed the sol-gel method to produce both pristine and boron-doped NiO thin films. They found that increasing the doping the level of boron in NiO thin films greatly influenced their optical properties, including the extinction coefficient, optical energy gap, dispersion energy, and refractive index [18]. However, there has been limited research on exploring the physical properties of $Ni_{1-x}Zn_xO$ thin films as hole transport layers (HTLs), particularly using the cost-effective and versatile spin coating technique. As a result, the study focused on examining the physical characteristics of both pure and Zn-doped NiO thin films, specifically in their role as hole transport layers.

2. Experimental work

Hydrated nickel acetate tetrahydrated ($Ni(OCOCH_3)_2{\cdot}4H_2O$), 2-methoxethanol ($C_3H_8O_2$), zinc acetate dehydrates ($Zn(CH_3COO)_2{\cdot}2H_2O$), and monoethanolamine (C_2H_7NO) were purchased from Sigma Aldrich with 99% average purity and used as the starting material, solvent, doping material, and stabilizer respectively, and as substrates, microscopic glass slides were used. First of all, the fixed amount of the $Ni(OCOCH_3)_2{\cdot}4H_2O$ and varying amounts (0, 0.0.05, 0.07, and 0.09) of the $Zn(CH_3COO)_2{\cdot}2H_2O$ were dissolved in the solvent via continuous stirring to prepare the four sample solutions. When all the precursors dissolved, few drops of the C_2H_7NO were added into the solution to make the solutions stable and transparent. After aging the solutions for 24 hours, they were then applied onto the ultrasonically cleaned glass slides (substrates) placed in the cabin of spin coater with the help of a dropper. These coated glass slides then dried using a hot plate for ten minutes at 100 °C. The whole deposition operation was repeated six times. Finally, the deposited glass slides were annealed for one hour in a furnace at 300 °C to obtain the required thin films. Table 1 provides a comprehensive details of deposition parameters.

2.1. Characterizations

The thickness was estimated using an accurate, easy, inexpensive mass difference approach [19]. The average thickness of NiO thin films has been estimated 300 nm. The XRD analysis using CuKα source radiations [20] analyzed the macro-structural properties of the $Ni_{1-x}Zn_xO$ films. FTIR analysis validated the successful deposition of the $Ni_{1-x}Zn_xO$ nano-particles [21] on the surface of glass slides (substrates). Moreover, the surface structure of the films was analyzed at the micro-scale level using scanning electron microscopy [22]. A UV-vis spectrophotometer recorded the optical absorption spectra ranging between 200 and 800 nm [23].The electrical characteristics (conductivity, carrier density, resistivity, and mobility) of $Ni_{1-x}Zn_xO$ thin films were analyzed using Hall effect

measurements. These measurements were conducted at room temperature by applying 1 nA current, 0.5 T magnetic strength, and 5 V potential with a 5S delay interval.

Table 1. Details of deposition parameters for the fabrication of $Ni_{1-x}Zn_xO$ thin films.

Parameter name	**Range/Value**
Substrate thickness	1 mm to 1.2 mm
Solution dropped on substrate	Approximately 1ml on each repetition
Spinning speed (rpm)	2500
Deposition temperature	Room temperature
Drying time	10 minutes
Drying temperature	100 ℃
Annealing Temperature	300 ℃
Annealing time	1 hour

3. Results and discussions

3.1. X-ray diffraction analysis

Figure 1 shows how we employed XRD measurement to investigate crystallinity of $Ni_{1-x}Zn_xO$ thin films. A minor diffraction peak represents the (200) planes, at 43.3° (Card No. 00-047-1049), in the prepared thin films belongs to NiO, and no more visible peaks appear as doping concentration increases, which could account for the preference for the (200) orientation. Many dismissed peaks are observed from 20º to 40º, indicating the amorphous phases of the particles deposited on glass slides used as substrates [24].

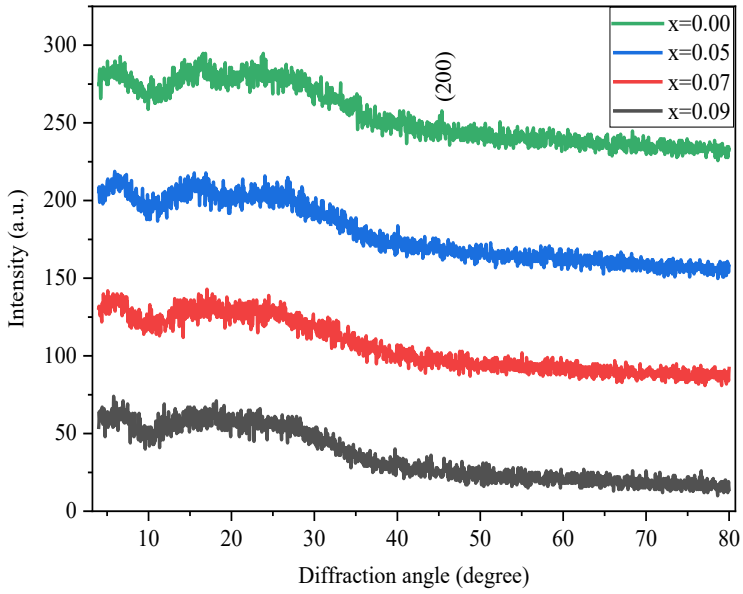

Fig. 1. XRD plots of $Ni_{1-x}Zn_xO$ thin films.

The XRD spectra of zinc-doped thin films show that (200) peaks are broad and low-intensity, which shows the poor crystalline structure of zinc-doped thin films. The drop in the peak intensity via zinc doping is in accordance with a previous research report [25]. The amorphous structure is observed in all $Ni_{1-x}Zn_xO$ thin films but more in zinc-doped NiO thin films. The absence of a well-defined fine structure or inadequate crystallinity in Zn-doped NiO could also be attributed

to the poor oxygen molecule desorption occurred that during the precursor stage [26]. It should be noted that the width of the optimal peak (200) increases as zinc concentration increases, indicating a decrease in crystallinity. It is also observed that doping the NiO films causes a minor shift from initial position of the optimal diffraction (200) peaks towards lower 2θ angles, indicating the possible conductivity change from p-type to n-type. The decrease in the intensity, increase in the width, and shifting of the peak (200) to smaller angle also indicate large crystallite size in tens [27]. According to previously reported literature, moderately large crystallite-size nanoparticles are required in solar cell applications. So, these moderately large crystallite size nanoparticles of the nickel oxide (NiO) thin films can influence the surface morphology, optical characteristics, interface quality, and electrical conductivity, thereby contributing significantly to the solar cell performance, particularly where NiO is frequently utilised as a hole transport layer. Hence, thin films reported in this work offer themselves as suitable HTLs, especially the pure NiO thin film with better crystallinity.

3.2. Fourier-transform infrared spectroscopy analysis

Fourier-transform infrared spectroscopy (FTIR) is frequently used to study microstructural changes in response to processing parameters like doping concentration. It mainly aids in the identification of functional groups found in thin films [28]. In FTIR analysis, we scanned the wavelength range from 4000 to 400 cm^{-1}, and determined the type of functional groups for specific bonds such as C-O, O-H, and Ni–O. Figure 2 shows FTIR spectra, which reveals the strong dependence of microstructural changes occurring in thin films due to the zinc doping and validates the presence of Ni-O bond indicating the successful preparation of pure and zinc-doped nickel oxide thin films. The FTIR spectra of the pure NiO shows four prominent bending peaks at 456 cm^{-1}, 762 cm^{-1}, 896 cm^{-1}, and 1063 cm^{-1}. A specific band region 400 to 800 cm^{-1} is assigned to Ni–O band, where the Ni–O stretching is indicated twice at 450 and 762 cm^{-1} for the pure NiO thin film [29]. Table 2 shows a comparison that validates the Ni-O bending.

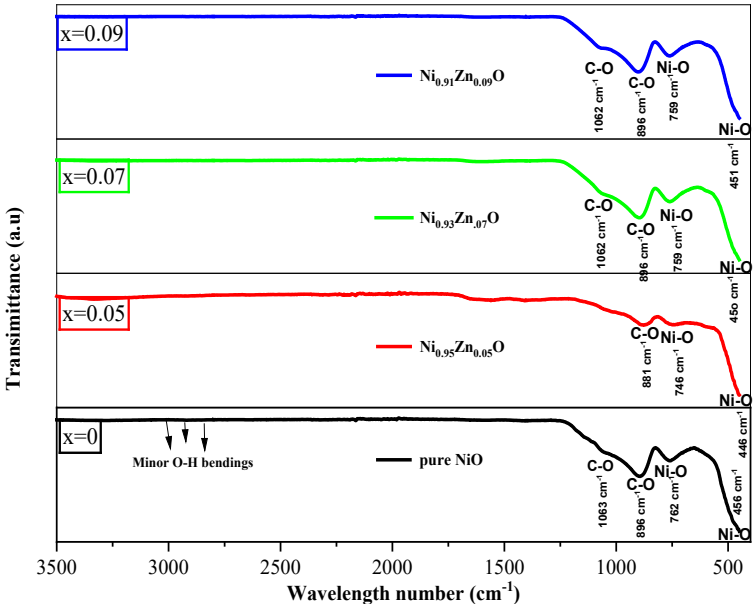

Fig. 2. Transmittance patterns of $Ni_{1-x}Zn_xO$ thin films.

The bands at 896 cm^{-1} and 1063 cm^{-1} are attributed to C-O stretching vibration [30, 31]. The bands in region 3151 cm^{-1} to 2835 cm^{-1} belong to O-H group. The pure NiO thin film sample shows a shift of the first Ni-O bending from 456 cm^{-1} to a lower wave number of 446 cm^{-1} as the concentration (x) reaches 0.05, as observed from Figure 2. It is also noted the intensity of the bending peaks reduce significantly for the sample where x = 0.05. Additionally, Ni-O bending appears at 450 cm^{-1}, 451cm^{-1} for the samples $Ni_{0.93}Zn_{0.07}O$ and $Ni_{0.91}Zn_{0.09}O$, respectively. The second Ni-O

stretching also shows a similar behaviour of shifting the peak (762 cm^{-1} to 746 cm^{-1} to 759 cm^{-1} to 759 cm^{-1}) to lower wavenumber. The shifting of the Ni-O bands at 446 cm^{-1} and 762 cm^{-1} peaks is in line with literature [32]. The C-O stretching experiences a shift from 896 cm^{-1} to 881 cm^{-1} with 0.05 doping, while no shift is observed for the next higher levels of doping. It is noticed that no prominent bending for O-H is observed, making the thin films acceptable as HTLs for application in perovskite solar cells because NiO thin films without or with minimal intensity O-H peaks are more transparent, allowing better light to reach the active layer in solar cells. This improved transparency is crucial in optimizing the light absorption, increasing the overall efficiency of the solar cell. The presence of hydroxyl groups in NiO films can cause instability, particularly in humid conditions or at high temperatures. The NiO thin film lacking O-H groups has higher thermal and chemical stability. This benefits solar cells, especially in outdoor environments where the exposure to sunshine and changing environmental conditions can cause materials to degrade over time. In addition to this, the presence of hydroxyl groups (O-H) in the NiO thin films can cause the defects or increase the charge carrier trapping sites, limiting charge mobility. NiO films without O-H groups exhibit increased hole conductivity by reducing these defect states, resulting in more efficient charge transport, facilitating the passage of the holes toward the electrodes and reducing recombination losses. Hence these thin films with minimal O-H groups can be used as hole transport layers.

Table 2. Comparison of the Ni-O stretching/bending.

Band position (cm^{-1})	Assigned group or stretching/ bending	Reference
415, 635	Ni-O	[32]
436	Ni-O	[33]
476	Ni-O	[34]
451, 719, 765, 775	Ni-O	[35]
450, 757, 896	Ni-O	Present work

3.3. Ultra violet – visible spectroscopy

3.3.1. Transmission spectra

Optical spectra are taken in transmittance mode using a UV-visible spectrophotometer. Figure 3 shows variations in the transmittance percentage for the $Ni_{1-x}Zn_xO$ thin films across 450 to 800 nm wavelength range.

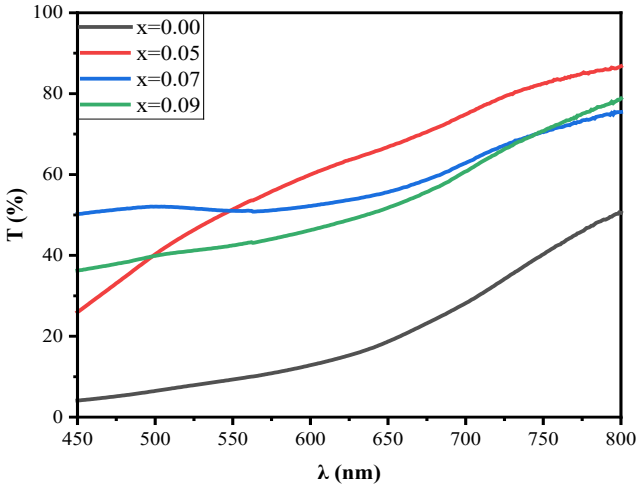

Fig. 3. Transmission patterns of $Ni_{1-x}Zn_xO$ thin films.

The optical transmittance is negligible in the [20] ultraviolet (UV) region for all thin films but increases in the visible region. An increase in zinc content up to 0.05, results in an increase from 50.5 to 87 % of transmittance within the visible region, while the transmittance drops to 77 % as x increases up to 0.07, and finally it increases up to 79% for the sample $Ni_{0.91}Zn_{0.09}O$. FTIR plots show that zinc enhances the transmittance greatly, indicating tuning of the band gap. Such enhancements in the transmittance results in less dispersion and fewer defects in thin films. The efficiency of solar cells can be greatly impacted by both parasitic absorption and light losses, which can be minimized by employing thin films showing less dispersion and high transmittance. This feature is essential to select a layer as HTL for the perovskite solar cells. Therefore, these less dispersive and less defective $Ni_{1-x}Zn_xO$ films can be offered to be used in perovskite solar cells as hole transport layers depending upon band gap value.

3.3.2. Band gap energy

The band gap energy represents a fundamental characteristic of semiconductors, it is the energy gap between the highest occupied and lowest vacant molecular orbitals. This differential energy level is crucial in determining the electrical and optical properties of a material. Tauc's relation, which comprises the absorption coefficient (α) and the transition frequency (v), can be applied to find an energy band gap (E_g) for a particular transition in the film. Direct permissible transitions for the NiO material, which has a direct band gap, were set to a value of 1/2 for n. The band gap was computed by drawing a straight line along the linear region of the $(\alpha hv)^2$ curves pointing to the energy axis, as illustrated in the figure 4. The band gap increases from 3.88 eV to 3.90 eV to 3.96 eV, and finally to 3.98 eV by 0 to 0.05, 0.05 to 0.07, and 0.07 to 0.09 doping concentrations, and is in line to literature [32, 36, 37]. The optical results of this study show that adding zinc can significantly change the band gap of NiO thin films. A low bandgap material is needed to prepare the hole transport layer because the unique formation of localized orbitals of low bandgap materials facilitates charge transportation and ensures better light absorption. Therefore, the pure NiO thin film with a low band gap of 3.88 eV looks more appealing for use as a hole transport layer than other thin films. Table 3 compares of band gap optimization between this work and different reports on zinc doped thin films.

$$(\alpha hv)^{1/n} = \beta(hv - E_g) \tag{1}$$

where symbol "β" is a constant indicates band tailing.

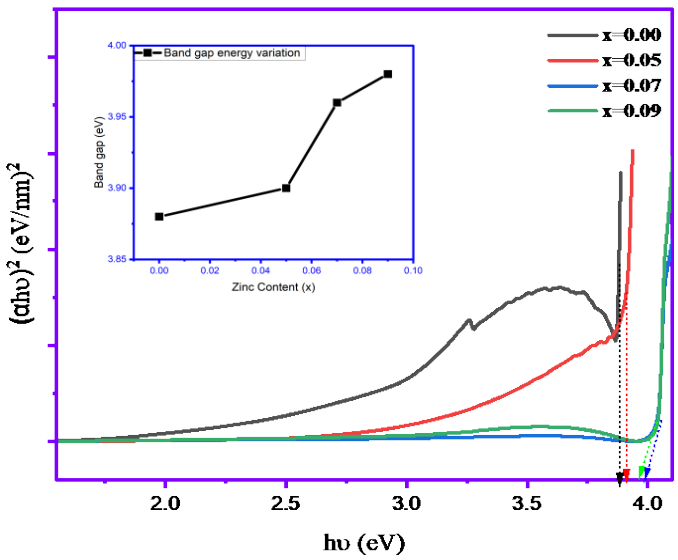

Fig. 4. Plots of $(\alpha hv)^2$ vs incident light energy (hv); Inset, Band gap variation vs zinc concentrations (x).
Table 3. Bandgap NiO thin films for various zinc concentrations.

Deposition Method	Zinc content	Band gap energy (eV)	Reference
Spray pyrolysis	0 – 6%	3.25 – 3.49	[37]
Sol-gel spin-coating	0 – 5%	3.76 – 3.93	[32]
Sol-gel spin-coating	0 – 10%	3.96 – 4.00	[12]
Chemical spray pyrolysis	0 – 4%	3.66 – 3.67	[20]
Sol-gel spin-coating	0 – 5%	3.95 – 3.95	[3]
Sol-gel spin-coating	0 – 4%	3.33 – 3.59	[15]
Spin coating	0 – 9% or (0 - 0.09)	3.88 – 3.98	Present work

3.4. SEM analysis

When thin films are utilised as a hole transport layer (HTL), their morphology is critical to the operation of electrical devices such perovskite solar cells and light-emitting diodes. A continuous, pinhole-free thin layer is required to completely cover the substrate and prevent short circuits in the device. A homogeneous coating contributes to long-term stability by preventing degradation in the device. Additionally, a compact and well-organized structure can act as a barrier against moisture and oxygen, effectively extending the lifespan of delicate devices such as perovskite solar cells. In Figure 5, SEM pictures of $Ni_{1-x}Zn_xO$ thin films are displayed with a magnification of 500.

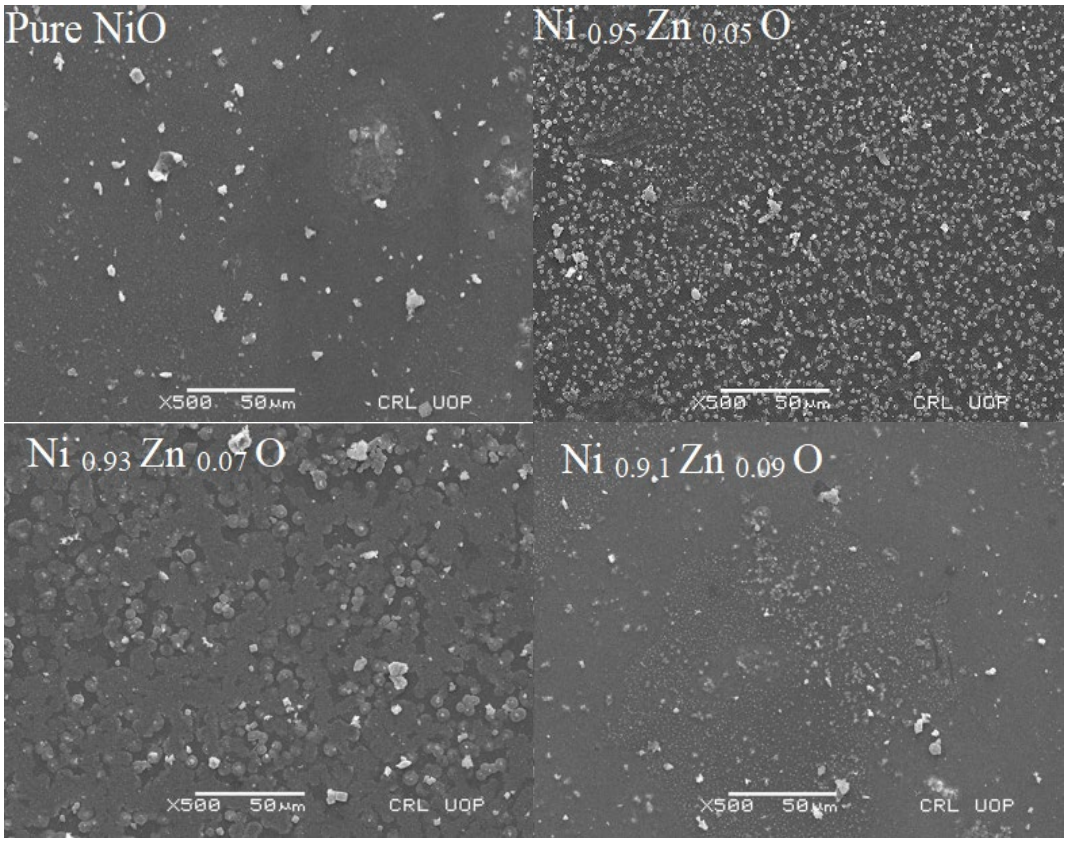

Fig. 5. SEM surface views of thin films doped at different concentrations.

The SEM picture of the pure NiO thin film demonstrates an even distribution across the glass substrate, indicating a crack-free, homogeneous, smooth, and well-adhered deposition." of the thin film. Furthermore, there are no apparent pinholes, indicating high film quality. The SEM image of the $Ni_{0.95}$ $Zn_{0.05}$ O thin film shows the existence of nano-sized particles dispersed across the glass

substrate, with small gaps in between them. The SEM picture of the $Ni_{0.93}Zn_{0.07}O$ thin film shows an evident improvement in particle agglomeration of moderate size nanoparticles. The SEM image of the $Ni_{0.91}Zn_{0.09}O$ thin film closely similar to that of the pure NiO thin film, revealing a well-adhered covering to the substrate with no gaps or cracks. When investigating the effect of zinc, one notable observation is the reduction in particle size within the $Ni_{0.95}Zn_{0.05}O$ thin film compared to all other films. Increasing the doping up to a level where x = 0.07 results in a notable increase in particle size, which could be ascribed to the successful incorporation of zinc into the NiO. Hence SEM analysis shows that zinc doping changes the morphology of $Ni_{1-x}Zn_xO$ thin films. After carefully examining the SEM results, we found that the pure NiO thin film will work better as a thermally stable hole transport layer than zinc-doped thin films with desired features including, even distribution, minimal cracking, absence of pinholes, and a moderate particle size.

3.5. Electrical properties

To use the thin film as a hole transport layer, one must examine its conductivity type, resistivity, mobility, and carrier concentration through Hall effect measurements. The equation (2) is used to find the carrier concentration [38].

$$N = 1/e\mu\rho \tag{2}$$

where N, e, μ, and ρ are the carrier concentration, charge (1.6×10^{-19} C), Hall mobility, and resistivity respectively. All the data obtained from Hall analysis is presented in Table 4. The numerical signs (- and +) attached to the carrier concentration and Hall mobility values indicate conductivity type. The pure NiO exhibits p type conductivity. Therefore, the majority charge carriers are holes. While doping of the order 0.05 to 0.09 into the NiO lattice changes its conductivity to n-type as indicated by negative signs in Table 4. Therefore, the majority charge carries of zinc doped thin films are electrons. The p to n-type conductivity shift might be attributed to the Ni metal-rich phase that occurred after annealing the thin films at 300 ℃ [39]. The pure NiO thin film has low resistivity of 1.66×10^{-3} Ω.cm and is in line with resistivity value reported in the literature [40]. It decreases to 1.71×10^{-6} Ω.cm by the addition of 0.05 zinc in the pure NiO thin film. It remains as low as 10^{-6} for the $Ni_{0.93}Zn_{0.07}O$ and $Ni_{0.91}Zn_{0.09}O$ thin films. The observed mobility of the pure NiO thin film is 1.55×10^{4} $cm^2\ V^{-1}\ s^{-1}$ and which increases to 3.99×10^{7} $cm^2\ V^{-1}\ s^{-1}$ for the sample $Ni_{0.95}Zn_{0.05}O$. The mobility value again increases to 4.96×10^{7} $cm^2\ V^{-1}\ s^{-1}$ for the sample $Ni_{0.93}Zn_{0.07}O$, and finally decreases to 1.46×10^{7} $cm^2\ V^{-1}\ s^{-1}$. The reduction in the collisional energy loss of the particles with oxygen during their course towards the substrate surface may be attributed to the increase in mobility [41]. The pure NiO thin film has a carrier concentration of 2.43×10^{17} cm^{-3}. While by introducing the 0.05 zinc content increases the carrier concentration to 2.55×10^{17} cm^{-3}. From these results we conclude that pure NiO thin film having p-type conductivity with holes as majority charge carriers, good carrier concentration, good mobility, and low resistivity fits well for efficient hole extraction and their transportation to the electrode. Hence, pure NiO thin film is better choice for use as hole transport layer.

Table 4. Carrier concentration (N), mobility (μ), and resistivity (ρ) values of the $Ni_{1-x}Zn_xO$ thin films.

Sample	N (cm^{-3})	μ ($cm^2\ V^{-1}\ s^{-1}$)	ρ (Ω.cm)	Conductivity type
Pure NiO	2.43×10^{17}	1.55×10^{4}	1.66×10^{-3}	p-type
$Ni_{0.95}Zn_{0.05}O$	-9.16×10^{16}	-3.99×10^{7}	1.71×10^{-6}	n-type
$Ni_{0.93}Zn_{0.07}O$	-7.00×10^{16}	-4.96×10^{7}	1.80×10^{-6}	n-type
$Ni_{0.91}Zn_{0.09}O$	-2.55×10^{17}	-1.46×10^{7}	1.68×10^{-6}	n-type

4. Conclusions

Present work explores the doping effects of zinc on the structural, optical, morphological, and electrical properties of the $Ni_{1-x}Zn_xO$ thin films fabricated via spin-coating technique, demonstrating their potential as hole transport layers. XRD spectra showed that zinc-doped nickel oxide thin films had poor crystallinity than undoped NiO thin films. FTIR study validated the presence of an Ni-O bond at 456 cm^{-1}, 446 cm^{-1}, 450 cm^{-1}, 451 cm^{-1}, 762 cm^{-1}, 746 cm^{-1}, 759 cm^{-1}, and 759 cm^{-1}. UV visible spectra showed that the band gap increased from 3.88 eV to 3.90 eV, then increased to 3.96 eV, and finally increased to 3.98 eV by 0.05, 0.07, 0.09 doping concentrations. With the increase of the zinc concentration, the optical transmittance increased from 55.5% to 87% as doping level reached 0.05, and finally to 79% for x = 0.09. Hall measurements revealed that p-type conductivity of the pure NiO thin film shifted to n-type conductivity for each doping level of zinc. A significant decrease in resistivity was found from 1.66×10^{-3} Ω.cm to 1.71×10^{-6} Ω.cm for the 0.05 zinc concentration and finally decreased to 1.68×10^{-6} Ω.cm for 0.09 zinc concentration.

The Hall measurements also revealed an increase in the hole mobility at each successive doping level up-to 0.07, and finally decreased to 1.46×10^{7} $cm^2 V^{-1} s^{-1}$. Although, the addition of 0.09 zinc content causes the carrier concentration to increases from 2.43×10^{17} cm^{-3} to 2.55×10^{17} cm^{-3} while conductivity still remains n-type. All the results confirmed that zinc doping affects the physical properties significantly. However, the pure NiO thin film showed better physical properties, including good crystallinity, a slightly lower band gap than zinc doped thin films, and uniform morphology. Additionally, p-type conductivity and a good carrier concentration of 2.43×10^{17} cm^{-3} were also demonstrated by the pure NiO thin film. The studied p-type thin films are appropriate for employment as a hole transport layer in perovskite solar cells.

Acknowledgements

As part of the National Research Program for Universities (NRPU), the authors would like to express their gratitude to the Higher Education Commission (HEC) for the financial support under project number "10304/Punjab/NRPU/R&D/HEC/2017"

Declaration of Competing Interest

The authors have no financial or personal interest that could in any way influence the findings of this work.

Funding statement

This work has received financial support solely from the Higher Education Commission Pakistan (Project Number "10304/Punjab/NRPU/R&D/HEC/2017").

Ethics statement

The authors affirm their commitment to comply with the publisher's ethical policy.

References

[1] Q. Fu, et al., ACS Energy Letters, 7(3), 1128-1136, (2022); https://doi.org/10.1021/acsenergylett.1c02812

[2] M. Saliba, et al., Chemistry of Materials, 30(13), 4193-4201, (2018); https://doi.org/10.1021/acs.chemmater.8b00136

[3] P.S. Thiruchelvan, et al., Coatings, 11(6), 627, (2021); https://doi.org/10.3390/coatings11060627

[4] M. Aftab, et al., Optical Materials, 119, 111369, (2021); https://doi.org/10.1016/j.optmat.2021.111369

[5] X. Xu, et al., Applied Surface Science, 550,149316, (2021); https://doi.org/10.1016/j.apsusc.2021.149316

[6] D. Kaya,etal., Thin SolidFilms, 732,138800, (2021); https://doi.org/10.1016/j.tsf.2021.138800

[7] R. Poulain, et al., ACS Applied Electronic Materials, 4(6), 2718-2728, (2022); https://doi.org/10.1021/acsaelm.2c00230

[8] M. Napari, et al., InfoMat, 3(5), 536-576, (2021); https://doi.org/10.1002/inf2.12146

[9] M.H. Mamat, et al., Journal of Electrical and Electronic Systems Research (JEESR), 16, 100-105, (2020); https://doi.org/10.24191/jeesr.v16i1.015

[10] N.R. Aswathy, et al., Materials Chemistry and Physics, 282, 125916, (2022); https://doi.org/10.1016/j.matchemphys.2022.125916

[11] W. Guo, et al., Materials Letters, 92, 291-295, (2013); https://doi.org/10.1016/j.matlet.2012.10.109

[12] K.H. Kim, et al., International Journal of Electrochemical Science, 15(5), 4065-4071, (2020); https://doi.org/10.20964/2020.05.28

[13] I. Manouchehri, et al., Optik, 127(20), 9400-9406, (2016); https://doi.org/10.1016/j.ijleo.2016.06.092

[14] M.B. Amor, et al., Materials science in semiconductor processing, 27, 994-1006, (2014); https://doi.org/10.1016/j.mssp.2014.08.008

[15] T. Sen, et al., Journal of Alloys and Compounds, 889, 161613, (2021); https://doi.org/10.1016/j.jallcom.2021.161613

[16] F. Wang, et al., Materials Science in Semiconductor Processing, 151, 106986, (2022); https://doi.org/10.1016/j.mssp.2022.106986

[17] Y.R. Denny, et al., Thin Solid Films, 591, 255-260, (2015); https://doi.org/10.1016/j.tsf.2015.04.043

[18] H. Aydin, et al., Journal of sol-gel science and technology, 64, 728-733, (2012); https://doi.org/10.1007/s10971-012-2909-1

[19] A.M. Koshy, et al., Physica B: Condensed Matter, 650, 414452, (2023); https://doi.org/10.1016/j.physb.2022.414452

[20] M.E. Begum, et al., Heliyon, 10(1), (2024); https://doi.org/10.1016/j.heliyon.2024.e39254

[21] U.K. Panigrahi, et al., Journal of Alloys and Compounds, 833, 155050, (2020); https://doi.org/10.1016/j.jallcom.2020.155050

[22] K. Gangareddy,et al., Journal of Materials Science, 35(6), 408, (2024); https://doi.org/10.1007/s10854-024-12135-0

[23] Noonuruk, R., et al., physica status solidi (c), 12(6), 560-563, (2015); https://doi.org/10.1002/pssc.201400303

[24] Y. Li, et al., Materials Research Bulletin, 44(6), 1232-1237, (2009); https://doi.org/10.1016/j.materresbull.2009.01.009

[25] M.H. Mamat, et al., Materials Research Bulletin, 127, 110860, (2020); https://doi.org/10.1016/j.materresbull.2020.110860

[26] N.F.Q. Fahmi, et al., Journal of Eectrical and Electronic System Research, 100-105, (2020); https://doi.org/10.24191/jeesr.v16i1.015

[27] N. Parimon, et al., Conf. Ser. Earth Environ. Sci, 682, 012070, (2021); https://doi.org/10.1088/1755-1315/682/1/012070

[28] P. Innocenzi, Journal of non-crystalline solids, 316(2-3), 309-319, (2003); https://doi.org/10.1016/S0022-3093(02)01637-X

[29] X.H. Huang, et al., Electrochemistry Communications, 10(9), 1288-1290, (2008); https://doi.org/10.1016/j.elecom.2008.06.020

[30] B.K. Mohammed, et al., Journal of Sol-Gel Science and Technology, 99, 1-12,

[31] N.V. Srinivasa, et al., Materials Today: Proceedings, 92, 1431-1437, (2023); https://doi.org/10.1016/j.matpr.2023.05.597

[32] S. Benhamida, et al., Dig. J. Nanomater. Biostruct, 16, 433-442, (2021);

[33] S. Dewan, et al., journal of applied physics, 121, 21, (2017); https://doi.org/10.1063/1.4984580

[34] B.J. Rani, et al., Journal of Sol-Gel Science and Technology, 89, 500-510, (2019); https://doi.org/10.1007/s10971-018-4886-5

[35] S. Minisha, et al., Water, 16(2), 340, (20240); https://doi.org/10.3390/w16020340

[36] C. Zaouche, et al., Digest Journal of Nanomaterials & Biostructures, 17(4), (2022);

[37] N. Pothukanuri, et al., Chemical Physics Impact, 8, 100397, (2024); https://doi.org/10.1016/j.chphi.2023.100397

[38] Y. Reddy, et al., Journal of nano- and electronic physics, 4(4), 04002 (2012)

[39] C. Park, et al., Applied Science and Convergence Technology, 24(3), 72-76, (2015); https://doi.org/10.5757/ASCT.2015.24.3.72

[40] P. Gupta, et al., Journal of Applied Physics, 111(1), (2012); https://doi.org/10.1063/1.4718579

[41] T.K. Yong, T. et al., Applied surface science, 248(1-4), 388-391, (2005); https://doi.org/10.1016/j.apsusc.2005.03.093